Quantum confinement dependence of the energy splitting and recombination dynamics of A and B excitons in a GaN/AlGaN quantum well

F. Stokker-Cheregi*
Department of Lasers, NILPRP, Magurele, 077125 Bucharest, Romania

A. Vinattieri
Department of Physics and LENS, University of Florence, Sesto, I-50019 Fiorentino, Italy

E. Feltin, D. Simeonov, J.-F. Carlin, R. Butté, and N. Grandjean
Institute of Quantum Electronics and Photonics, Ecole Polytechnique Fédérale de Lausanne, CH-1015 Lausanne, Switzerland

F. Sacconi, M. Povolotskyi, and A. Di Carlo
Department of Electronic Engineering, University of Rome "Tor Vergata," 00133 Rome, Italy

M. Gurioli
Department of Physics and LENS, University of Florence, Sesto, I-50019 Fiorentino, Italy
(Received 31 March 2009; published 18 June 2009)

We report the observation of well-resolved A and B excitonic resonances in the reflectivity spectra of a wedged GaN/AlGaN quantum well (QW) with 5% Al content in the barriers for different well thicknesses. For the thicker well cases, the energy splitting between the A and B excitons is larger than the one found for bulk GaN. However, the A-B exciton energy splitting decreases with decreasing well thickness, accordingly to the delocalization of the electron and hole wave functions in very thin QWs, as supported by theoretical simulations. Moreover, we used time-resolved photoluminescence measurements to investigate the recombination dynamics of the two excitonic states demonstrating the existence of a thermodynamic equilibrium between the two populations at a sample temperature of 10 K.

DOI: 10.1103/PhysRevB.79.245316 PACS number(s): 78.47.−p, 78.55.Cr, 71.35.−y

I. INTRODUCTION

The field of III-nitride semiconductors has been the subject of an extensive number of studies over the past two decades.[1] Gallium nitride (GaN), in particular, exhibits a wideband gap (~3.5 eV at $T=4$ K) and luminescence properties that make it the leading material for UV-visible optoelectronic applications. In fact, GaN and its related alloys are nowadays successfully incorporated in devices ranging from light emitting diodes that cover the entire visible spectrum to state-of-the-art commercial data storage devices such as the Blu-ray disk. Recently, a remarkable effort, driven by the technological importance of spin-based electronics (so-called spintronics), has been devoted to the understanding of spin-relaxation processes between all the excitonic features[2,3] (called A, B, and C excitons)[4] arising from the valence-band splitting due to the crystal-field and the spin-orbit interactions.

The interest in GaN/AlGaN quantum wells (QWs) was sparked, among other things, by the increased exciton binding energy in these systems with respect to bulk GaN. In fact, the exciton binding energy on the order of 45–50 meV in low Al content narrow GaN/AlGaN QWs (Ref. 5) makes these heterostructures an interesting choice for the realization of UV lasers and polariton lasers[6] operating at room temperature. However, until recently, the lattice-mismatch-induced strain and structural defects proved to be a great challenge for the growth of these heteroepitaxial structures, and the optical quality of the active QW region was still much lower than that achieved for GaN epilayers. While for bulk GaN the separate features of A, B, and C excitons have been clearly observed in both reflectivity and photoluminescence (PL) measurements,[7–9] effects such as the presence of a strong internal electric field and the broadening of the emission lines due to alloy composition fluctuations in the barriers and/or interface roughness have long hindered the observation of similar fine excitonic structures in GaN/AlGaN QWs.[10,11]

In this work, we report the observation of the A (X_A) and B (X_B) excitons in the low-temperature ($T=10$ K) reflectivity and PL spectra of a narrow-wedged high-quality $GaN/Al_{0.05}Ga_{0.95}N$ QW, for which we have previously analyzed the biexciton (BX) properties.[12] The effect of quantum confinement on the A-B excitonic splitting is investigated and a model is used to account for its variation with the well thickness. We also used time-resolved (TR) PL measurements under nonresonant and X_A resonant excitation to investigate the recombination dynamics of the two excitonic states and their interaction.

II. EXPERIMENT

The single GaN QW was grown by metal organic vapor phase epitaxy on a buffer layer consisting of a high-quality 3-μm-thick GaN template deposited on c-plane sapphire followed by a 200-nm-thick $Al_{0.05}Ga_{0.95}N$ layer. It was then capped with a 50-nm-thick $Al_{0.05}Ga_{0.95}N$ layer. A detailed description of the growth process and optimization of the

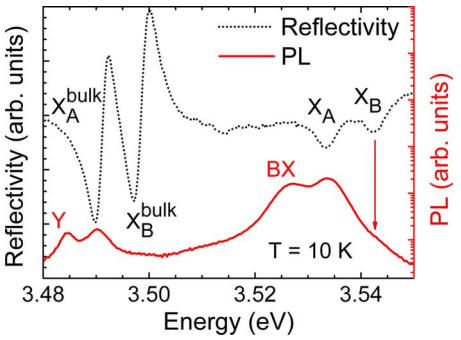

FIG. 1. (Color online) Reflectivity (dotted line) and photoluminescence (solid line) spectra taken at the same point of the $GaN/Al_{0.05}Ga_{0.95}N$ QW at $T=10$ K. On the higher energy side of the plot, X_A (X_B) designates the A (B) exciton feature of the QW while BX refers to the biexciton emission from the QW observable only in PL. On the lower energy side of the plot, features of the GaN buffer layer can be seen.

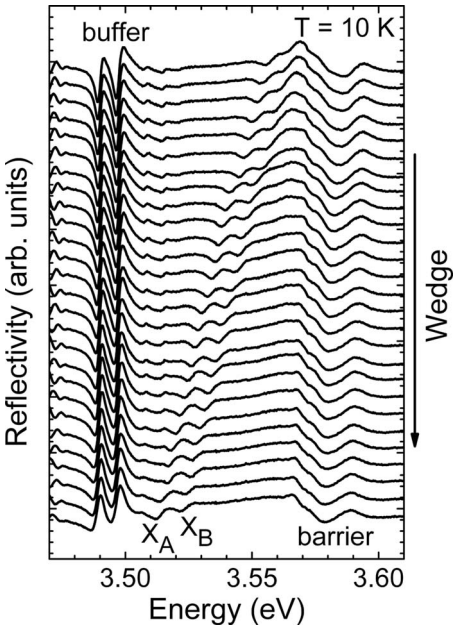

FIG. 2. Reflectivity spectra taken at different positions across the well thickness gradient of the $GaN/Al_{0.05}Ga_{0.95}N$ QW at $T=10$ K. While the energies of X_A and X_B vary, the features corresponding to the GaN buffer layer (buffer) and $Al_{0.05}Ga_{0.95}N$ barriers (barrier) remain unchanged. The spectra are shifted in intensity for the sake of clarity.

interfaces is provided in Ref. 13. The growth was conducted so as to produce a thickness gradient of the well region across the sample leading to an accessible thickness which varies from 1.5 to 2.9 nm. As a result, the energy of the exciton recombination can be efficiently tuned on the same sample. Reflectivity measurements were performed using a Xe lamp. Time-integrated photoluminescence measurements were carried out under nonresonant excitation using the second harmonic generation of a synchronously pumped dye laser with 8 ps pulses at 300 nm with a repetition rate of 76 MHz. The collected light was detected by a silicon charge-coupled device camera after dispersion through a 50-cm-flat field monochromator. TR PL measurements were performed using a mode-locked Ti:sapphire laser pumped by a continuous wave Ar^+ laser providing 1.2 ps pulses at a repetition rate of 81 MHz. The second harmonic (350 nm) and third harmonic (270 nm) of the Ti:sapphire laser have been used for resonant and nonresonant excitations, respectively. The PL was dispersed through a 30-cm-flat field monochromator and detected by a streak camera apparatus with a 3 ps time resolution. All measurements were performed at a sample temperature of 10 K with the sample placed in a closed cycle cryostat.

III. RESULTS AND DISCUSSION

In Fig. 1 we present the reflectivity (dotted line) and PL (solid line) spectra taken at the same position on the sample at $T=10$ K with X_A at 3.533 eV. Even though a line shape fit would be needed to extract the excitonic resonances in the reflectivity spectrum, the comparison with the PL spectrum shows a quite small (if any) Stokes shift between the reflectivity and the PL resonances, denoting small localization effects. While prominent features can be observed for X_A in both reflectivity and PL, X_B is quite visible in reflectivity whereas it only appears as a shoulder on the higher energy side of X_A (marked by the arrow) in PL likely due to thermalization effects. The presence of the BX in the QW emission spectra has been discussed elsewhere.[12] The features visible on the low-energy side of the reflectivity spectrum in Fig. 1 correspond to the A and B excitons of the GaN buffer layer. Finally, the lowest energy PL band marked as Y in Fig. 1 is ascribed (by means of power dependence) to two independent contributions, namely, the biexciton and the neutral donor bound exciton[14] of the GaN buffer layer, which spectrally overlap.

From the reflectivity spectrum displayed in Fig. 1, we extract a 7.3 meV energy splitting between the A and B excitons of the GaN buffer layer, a value which is consistent with those found by other authors for GaN layers grown on *c*-plane sapphire substrates.[3,8,9] However, the value extracted for the energy splitting between X_A and X_B corresponding to the QW amounts to 9.1 meV, which is a clear indication of the effect of quantum confinement on the energy splitting between these two excitons.

In order to extract the variation in the energy splitting between X_A and X_B with quantum confinement, we took advantage of the thickness gradient of the well region and we acquired several reflectivity spectra at different positions across the sample (Fig. 2). As expected, the energy positions of X_A and X_B increase with increasing quantum confinement whereas the energies of the GaN buffer features (buffer) and $Al_{0.05}Ga_{0.95}N$ barriers (barrier) remain unchanged. This proves that a change in quantum confinement is caused by a change in the well width and not by a variation in the barrier height (i.e., a variation in the Al content in the barriers).

Figure 3 shows the energy splitting between X_A and X_B, as extracted from the reflectivity spectra of Fig. 2, as a function of the energy position of X_A (circles). In the inset we report the values of the X_A binding energy (ΔE_{XA}), estimated from the experimental data of the biexciton binding energy

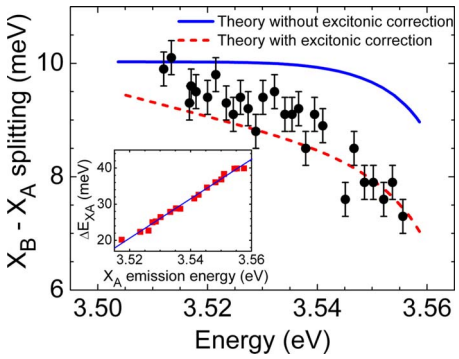

FIG. 3. (Color online) Energy splitting between X_A and X_B of the $GaN/Al_{0.05}Ga_{0.95}N$ QW as a function of the A exciton energy position (circles) as deduced from the reflectivity spectra in Fig. 2; the error bars refer to the experimental resolution. The theoretical fit to the experimental data for identical (different) X_A and X_B exciton binding energies is shown as a full (dashed) line. The X_A exciton binding energy estimated as described in the text and a linear fit are displayed in the inset.

as discussed in the next paragraph and a linear fit to the data. The clear enhancement of the energy splitting between the two excitons, with respect to the value of 7.3 meV measured in the GaN buffer layer, is attributed to the presence of quantum confinement in our QW and to the smaller in-plane mass of the light holes (X_B) with respect to the heavy holes (X_A). The impact of quantum confinement is stronger for X_B which has an energy state higher than X_A hence the increase in the energy splitting from 7.3 meV measured for our GaN buffer layer up to around 10 meV measured for the thicker well case (~2.9 nm) achieved in our wedged sample. Ideally, for carriers in a QW with infinite barriers, if one could neglect the influence of the strain, built-in field and excitonic effects, the X_B-X_A energy splitting should increase with increasing confinement (i.e., when reducing the well width). However, in our case, a decreasing energy splitting between X_A and X_B is observed showing that other important effects play a major role.

We calculated the theoretical energy splitting between X_A and X_B by using the TIBERCAD simulation tool.[15,16] In our calculations a strain model based on the continuous elasticity theory is applied,[17] which allows to include the effects of strain, piezo, and spontaneous polarization fields in the Poisson equation. Surface states have been taken into account by imposing a Fermi level pinning boundary condition to the AlGaN layer. Strain is calculated taking into account that the $GaN/Al_{0.05}Ga_{0.95}N$ heterostructure is grown on a GaN epilayer which exhibits a residual compressive stress of a few kilobar. By fitting the experimental value for the A exciton recombination (3.49 eV) of the GaN buffer epilayer we find a value of 3.7 kbar for this residual stress, which is then included in the simulation. The Al content in the barrier (x_{Al}) has been fitted in order to reproduce the experimental value of the X_A transition (3.57 eV) of the AlGaN layer, yielding x_{Al}=4.5%. The resulting conduction band offset (CBO) is 56 meV and the valence-band offset (VBO) is 24 meV if we consider a standard CBO to VBO ratio of 70:30. The confinement energy for electrons and holes are resolved, including in a self-consistent way the effects of strain, piezo, and spontaneous polarization fields, by using an eight-band $\boldsymbol{k}\cdot\boldsymbol{p}$ calculation[18] with the parameters reported in Ref. 19. The model includes both effects of strain and built-in self-consistent electric field in the Hartree approximation. The exciton transition energy is calculated as $E_X=E_c-E_h-\Delta E_{XA}$, where E_c and E_h are the eigenenergies of the confined electron and hole states, respectively. The calculations do not include excitonic effects but we can estimate the exciton binding energy contribution ΔE_{XA} from the experimental data presented in Ref. 12. From these data, and assuming for the Haynes factor[20] $f=\Delta E_{BX}/\Delta E_{XA}$ a value equal to 0.228, we can obtain the exciton binding energy as a function of the exciton emission energy, reported in the inset of Fig. 3. Note that ΔE_{XA} spans from 20 to 40 meV for the investigated QW.

The result of the simulation, assuming in a first approximation that the binding energies are the same for the two lowest transition energies (A and B excitons), is reported as a full line in Fig. 3. Simulated results reproduce nicely the experimental value of the X_B-X_A energy splitting of around 10 meV measured for the thicker well case (~2.9 nm) achieved in our wedged sample. Quantitatively, the variation in the theoretical splitting between X_A and X_B was found to be on the order of 3% when changing the CBO to VBO ratio between 75:25 and 68:32. We also note that for large quantum wells the energy splitting does not decrease toward its bulk value. This is due to the polarization-induced electric field which confines carriers, pushing electron and hole states toward opposite well edges. However, the theoretical predictions, in contrast with the experimental data, show a very flat dependence of the energy splitting between X_A and X_B with the QW thickness for the thicker well widths whereas for very small well widths a rapid decrease in the splitting is observed. This quick decrease in the X_B-X_A splitting in the simulated data, when decreasing the well thickness, is due to the fact that while the energies of both X_A and X_B increase, X_B approaches the barrier limit before X_A does so that the electron and hole wave functions for X_B are more sensitive to delocalization effects outside the well region making the overall energy enhancement due to the increase in quantum confinement smaller than for X_A.

As the theoretical calculations include all possible effects for the band to band transitions, we therefore conclude that the almost linear decrease in the experimental value of the energy splitting between X_A and X_B has to be ascribed to an excitonic effect. In particular, the hypothesis that the exciton binding energy is the same for the two lowest transition energies (A and B excitons) is rather crude. For instance, it is well known that in the case of GaAs QWs the heavy hole exciton has a smaller binding energy than the light hole exciton.[21] The X_B binding energy (ΔE_{XB}) can be estimated by considering the fact that in a hydrogenlike atom model, the Rydberg constant is proportional to the electron-hole-reduced mass, both for three-dimensional and two-dimensional excitons.[22] From the calculated in-plane dispersions we used a theoretical simulation to estimate the effective masses of electrons (m_e), heavy (m_{hA}), and light (m_{hB}) holes in the QW. The results are $m_e=0.205m_0$, $m_{hA}=0.45m_0$, and $m_{hB}=0.51m_0$, where m_0 is the free electron mass. Note that in the QW plane the heavy hole mass is

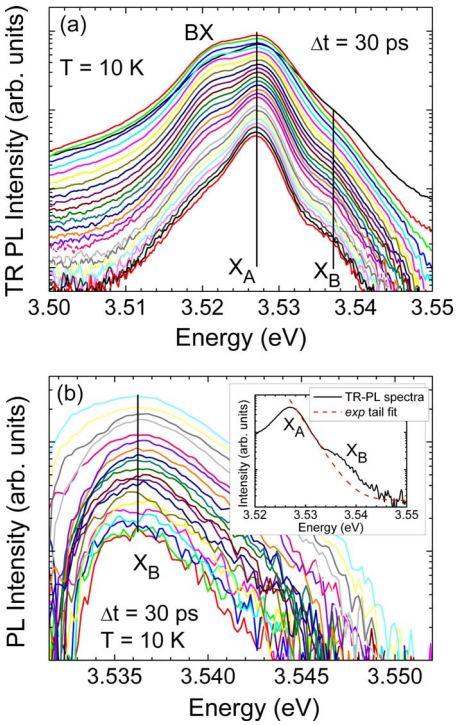

FIG. 4. (Color online) (a) TR PL spectra (in semilogarithmic scale) of the GaN/$Al_{0.05}Ga_{0.95}N$ QW with a time window and time steps of 30 ps taken at 10 K under nonresonant excitation with the laser at ~270 nm, using an incident power density of 80 W/cm^2. (b) TR PL spectra of the X_B recombination band extracted from Fig. 4(a) following the subtraction procedure illustrated in the inset (see text for details).

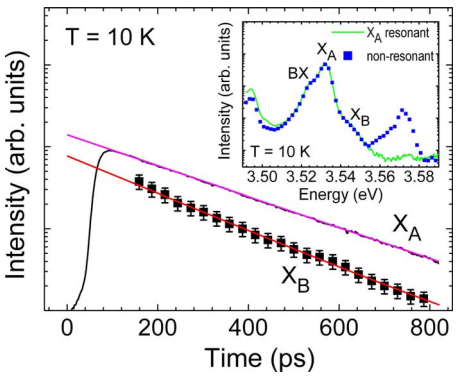

FIG. 5. (Color online) Decay profiles (in semilogarithmic scale) of the X_A (line) and X_B recombination bands (squares) and their respective exponential decay fits (straight lines). Intensities are shifted for the sake of clarity. The inset presents spectra acquired 200 ps after the excitation pulse using a time window of 250 ps for nonresonant (squares) and X_A resonant (line) excitations with intensities normalized to the X_A peak.

smaller than the light hole mass, a result that is similar with the findings on GaAs QWs.[21] Finally, ΔE_{XB} is obtained by scaling the experimental estimation for the A exciton binding energy ΔE_{XA} (full line in the inset of Fig. 3) by the ratio of the reduced masses $\Delta E_{XB}=\Delta E_{XA}(\mu_B/\mu_A)$. After recalculating the X_B transition energy we evaluated the energy splitting between X_A and X_B and the result is displayed as a dashed line in Fig. 3. It can be seen that this last theoretical curve, which includes excitonic effects, is in very good agreement with the experimental data.

Let us now discuss the recombination kinetics. In Fig. 4(a) we present TR PL spectra (corresponding to a point on the sample where the energy of the X_A recombination band is ~3.527 eV) obtained using a time window of 30 ps and an incident power density of 80 W/cm^2. In order to reduce the stray light in the TR PL measurements, especially relevant at short delays after the laser pulse, we used a slightly more nonresonant excitation (λ_{exc} ~ 270 nm). The X_B recombination is clearly visible as a shoulder on the higher energy side of the spectra, approximately 10 meV above the X_A band, a value estimated from reflectivity. It is also clear that the two excitons exhibit longer recombination times than the BX band which appears to decay faster.[12]

In order to deduce the X_B intensity at each time step, we subtracted an exponential tail that fits the shoulder of X_A from each of the TR PL spectra displayed in Fig. 4(a), as illustrated in the inset of Fig. 4(b). We point out that a background was added to the fitting of the exponential tail to account for the background signal in the PL spectra. The spectra resulting from this subtraction procedure are presented in Fig. 4(b). Despite the crudeness of our fitting procedure, we consider that the obtained TR PL bands give a fairly good estimate of the time evolution of the X_B recombination since its position and line broadening (~5 meV) are similar to those observed in reflectivity.

The time dependence of X_B intensities extracted from Fig. 4(b) is reported in Fig. 5 in semilogarithmic scale (squares). An exponential decay fit (line) yields a 190 ps (±30 ps) lifetime for the B exciton recombination band.[23] In Fig. 5 we also report the decay profile of the X_A band for comparison, which is found to have a lifetime of 230 ps (±5 ps) at this position on the sample, using an exponential decay fit. The similar decay times of the two exciton populations denote similar recombination kinetics. This can be attributed either to almost identical recombination kinetics of two noninteracting states or to the presence of an efficient population exchange between the two states. In order to gain further insight on this issue, additional PL measurements have been carried out using resonant excitation at the absorption energy of the A exciton in the QW. In the case of identical recombination kinetics of two noninteracting states we expect to observe, under resonant excitation, only the recombination from the A exciton. On the contrary, in the case of efficient population exchange, the X_B states must be populated by the photogenerated X_A excitons which acquire the X_B-X_A energy difference through phonon absorption, resulting in an anti-Stokes PL emission. The comparison between resonant (full line) and nonresonant (dotted line) TR PL spectra is presented in the inset of Fig. 5, normalized to the X_A peak intensity. The PL spectra were taken 200 ps after the excitation pulse in order to avoid contributions from the laser and resonant Rayleigh scattering, and were integrated over a time window of 250 ps. The emission from the AlGaN barrier is visible at high energy in the nonresonant spectrum while it is obviously missing in the resonant PL spectrum. The very good overlap between the QW emission lines for the non-

resonant (squares) and X_A resonant (line) spectra shown in the inset of Fig. 5 supports the hypothesis of an efficient population exchange, not only in the energy relaxation path but also in the up-conversion energy channel. Together with the similar lifetimes found for the two excitonic states, this demonstrates the presence of a thermodynamic equilibrium between the two populations.

IV. CONCLUSION

In conclusion, the remarkable observation of the B exciton recombination band in both reflectivity and PL in a $GaN/Al_{0.05}Ga_{0.95}N$ QW was made possible by its high optical quality, resulting in a small inhomogeneous broadening of the excitonic transitions and a reduced influence of the quantum confined Stark effect. Low-temperature reflectivity measurements performed on this $GaN/Al_{0.05}Ga_{0.95}N$ QW show an enhancement of the energy splitting between the A and B excitons, with respect to a bulk GaN layer, due to the presence of quantum confinement. However, with reducing the well width, the effect of the finite barriers causes a larger delocalization of the electron and hole wave functions of X_B, and, consequently, a reduction in the energy splitting between X_A and X_B, in very good agreement with theoretical simulations. Nonresonant and X_A resonant excitation PL measurements reveal that the X_A and X_B bands share similar recombination kinetics, as well as similar population distributions, indicating the existence of a thermodynamic equilibrium between the two states at a sample temperature of 10 K.

ACKNOWLEDGMENTS

This work was supported by NCCR Quantum Photonics (NCCR QP), research instrument of the Swiss National Science Foundation (SNSF), and SNSF Project No. 200020-122294.

*stokker@nipne.ro

[1] S. C. Jain, M. Willander, J. Narayan, and R. Van Overstraeten, J. Appl. Phys. **87**, 965 (2000).
[2] T. Ishiguro, Y. Toda, and S. Adachi, Appl. Phys. Lett. **90**, 011904 (2007).
[3] C. Brimont, M. Gallart, O. Crégut, B. Hönerlage, and P. Gilliot, Phys. Rev. B **77**, 125201 (2008).
[4] R. Dingle, D. D. Sell, S. E. Stokowski, P. J. Dean, and R. B. Zetterstrom, Phys. Rev. B **3**, 497 (1971).
[5] G. Christmann, R. Butté, E. Feltin, A. Mouti, P. A. Stadelmann, A. Castiglia, J.-F. Carlin, and N. Grandjean, Phys. Rev. B **77**, 085310 (2008).
[6] G. Malpuech, A. Di Carlo, A. Kavokin, J. J. Baumberg, M. Zamfirescu, and P. Lugli, Appl. Phys. Lett. **81**, 412 (2002); G. Christmann, R. Butté, E. Feltin, J.-F. Carlin, and N. Grandjean, *ibid.* **93**, 051102 (2008).
[7] B. Monemar, Phys. Rev. B **10**, 676 (1974).
[8] M. Tchounkeu, O. Briot, B. Gil, J. P. Alexis, and R.-L. Aulombard, J. Appl. Phys. **80**, 5352 (1996).
[9] D. Volm, K. Oettinger, T. Streibl, D. Kovalev, M. Ben-Chorin, J. Diener, B. K. Meyer, J. Majewski, L. Eckey, A. Hoffmann, H. Amano, I. Akasaki, K. Hiramatsu, and T. Detchprohm, Phys. Rev. B **53**, 16543 (1996).
[10] M. Esmaeili, M. Sabooni, H. Haratizadeh, P. P. Paskov, B. Monemar, P. O. Holz, S. Kamiyama, and M. Iwaya, J. Phys.: Condens. Matter **19**, 356218 (2007).
[11] F. Natali, D. Byrne, M. Leroux, B. Damilano, F. Semond, A. Le Louarn, S. Vezian, N. Grandjean, and J. Massies, Phys. Rev. B **71**, 075311 (2005).
[12] F. S. Cheregi, A. Vinattieri, E. Feltin, D. Simeonov, J. F. Carlin, R. Butte, N. Grandjean, and M. Gurioli, Phys. Rev. B **77**, 125342 (2008); F. Stokker-Cheregi, A. Vinattieri, E. Feltin, D. Simeonov, J. Levrat, J.-F. Carlin, R. Butté, N. Grandjean, and M. Gurioli, Appl. Phys. Lett. **93**, 152105 (2008).
[13] E. Feltin, D. Simeonov, J.-F. Carlin, R. Butté, and N. Grandjean, Appl. Phys. Lett. **90**, 021905 (2007).
[14] D. Martin, J. Napierala, M. Ilegems, R. Butté, and N. Grandjean, Appl. Phys. Lett. **88**, 241914 (2006).
[15] M. Auf der Maur, M. Povolotskyi, F. Sacconi, and A. Di Carlo, Superlattices Microstruct. **41**, 381 (2007).
[16] TIBERCAD simulation package, http://www.tibercad.org
[17] M. Povolotskyi and A. Di Carlo, J. Appl. Phys. **100**, 063514 (2006).
[18] S. L. Chuang and C. S. Chang, Phys. Rev. B **54**, 2491 (1996).
[19] I. Vurgaftman and J. R. Meyer, J. Appl. Phys. **94**, 3675 (2003).
[20] A. Thilagam, Phys. Rev. B **56**, 4665 (1997).
[21] L. C. Andreani and A. Pasquarello, Phys. Rev. B **42**, 8928 (1990).
[22] H. Haug and S. W. Koch, *Quantum Theory of the Optical and Electronic Properties of Semiconductors* (World Scientific, Singapore, 1994).
[23] The larger lifetime uncertainty of the B exciton with respect to the A exciton arises from the background subtraction procedure needed to extract the B exciton band.